CHAPTER 3: CRUSTAL MELTING: WORKING WITH ENCLAVES

Bernardo Cesare
Dipartimento di Geoscienze, Università di Padova
and C.N.R., Istituto di Geoscienze e Georisorse
Corso Garibaldi, 37, I-35137 Padova,
Italy
E-mail: bernardo.cesare@unipd.it

INTRODUCTION

In another chapter in this volume (Holness 2008), emphasis has been placed on the problems related to the recognition of microstructures indicating the presence of melt in migmatites, and on how these problems may be in part circumvented, for example by studying pyrometamorphosed rocks.

More generally, despite being by far the most important and voluminous witness of how the partially melted, deep levels of the crust should look like (review in Brown 2007), migmatites suffer from one major problem: their slow cooling. Grant (1985) nicely outlined that "*Although we have been discussing partial melting of pelitic rocks, more of what we now see in a pelitic migmatite is probably attributable to re-crystallisation*". In other words, migmatitic complexes mostly represent an anatectic product which has been affected by further modifications of microstructure (summary in Holness 2008), phase assemblage (*e.g.*, Kriegsman and Hensen 1998), phase composition (*e.g.*, Cesare *et al.* 2008) and physical properties (*e.g.*, Ferri *et al.* 2007).

Experimental studies (reviewed by Clemens 2006) provide considerable, essential information for the interpretation of migmatites, by reproducing the *P–T–X* conditions relevant for the partial melting of the mid to deep crust, and by defining, as a result, the main melting reactions, the chemistry of phases, the compositions of melts and the fertility of different parent rocks. However, owing to their small size, rapid run times and in some cases simplified chemical systems, experimental simulations cannot fully represent the behavior of natural anatectic environments, so that a significant gap in the knowledge of how partial melting actually takes place in nature remains.

In this chapter I will describe how metasedimentary enclaves in volcanic rocks (very rare although probably overlooked) may help fill the gap mentioned above. Brought to the surface from depths of *ca*. 20 km by volcanic eruptions, the rock fragments enclosed in the volcanic rocks of the Neogene Volcanic Province (NVP) of SE Spain can be considered as "natural experimental charges" (*e.g.*, Downes *et al.* 2004), because their rapid cooling has allowed the preservation of the anatectic melt as glass. Unlike the pyrometamorphic rocks referred to by Holness (2008) the enclaves described here have a much deeper origin, and an inferred genetic relation to the lavas in which they are hosted.

The enclaves in the volcanic rocks of the NVP have been extensively studied in the last decade (Cesare *et al.* 1997, 2002, 2003a, 2003b, 2003c, 2005, 2007, Cesare & Maineri 1999, Cesare 2000, Álvarez-Valero *et al.* 2005, 2007, Acosta-Vigil *et al.* 2007, Álvarez-Valero & Kriegsman 2007, Ferri *et al.* 2007) and the reader may refer to these papers for the details of their geology, petrology, mineralogy, geochronology and rock physics. Here I will review some of their main bearings for the petrogenesis of anatectic metapelite, focusing, unless specified, on the enclaves from the localities of El Hoyazo. Here one can observe two main types of enclaves: the Bt–Grt–Sil (Fig. 3-1a) and the Spl–Crd types (Fig. 3-1b). The former, more abundant in the field and most studied, is represented by well foliated, Qtz-free rocks consisting of Grt–Pl–Bt–Sil–Gph–glass±Ilm±Crd±Kfs±Spl (mineral abbreviations after Kretz 1983). The bulk composition of the enclaves is highly residual (*ca*. 44 wt.% SiO_2, 31% Al_2O_3, 10% FeO_{tot}), and their thermobarometric study indicates equilibration temperature of 850±50°C and pressure of 5–7 kbar. According to Cesare *et al.* (1997), these rocks represent the residue (restite) after anatexis of graphitic metapelite and extraction of 40–60 wt.% granitic melt, contaminated by mafic magmas (Benito *et al.* 1999) and now represented by the host dacite.

Mineralogical Association of Canada Short Course 38, Quebec City, Quebec, p. 37-55

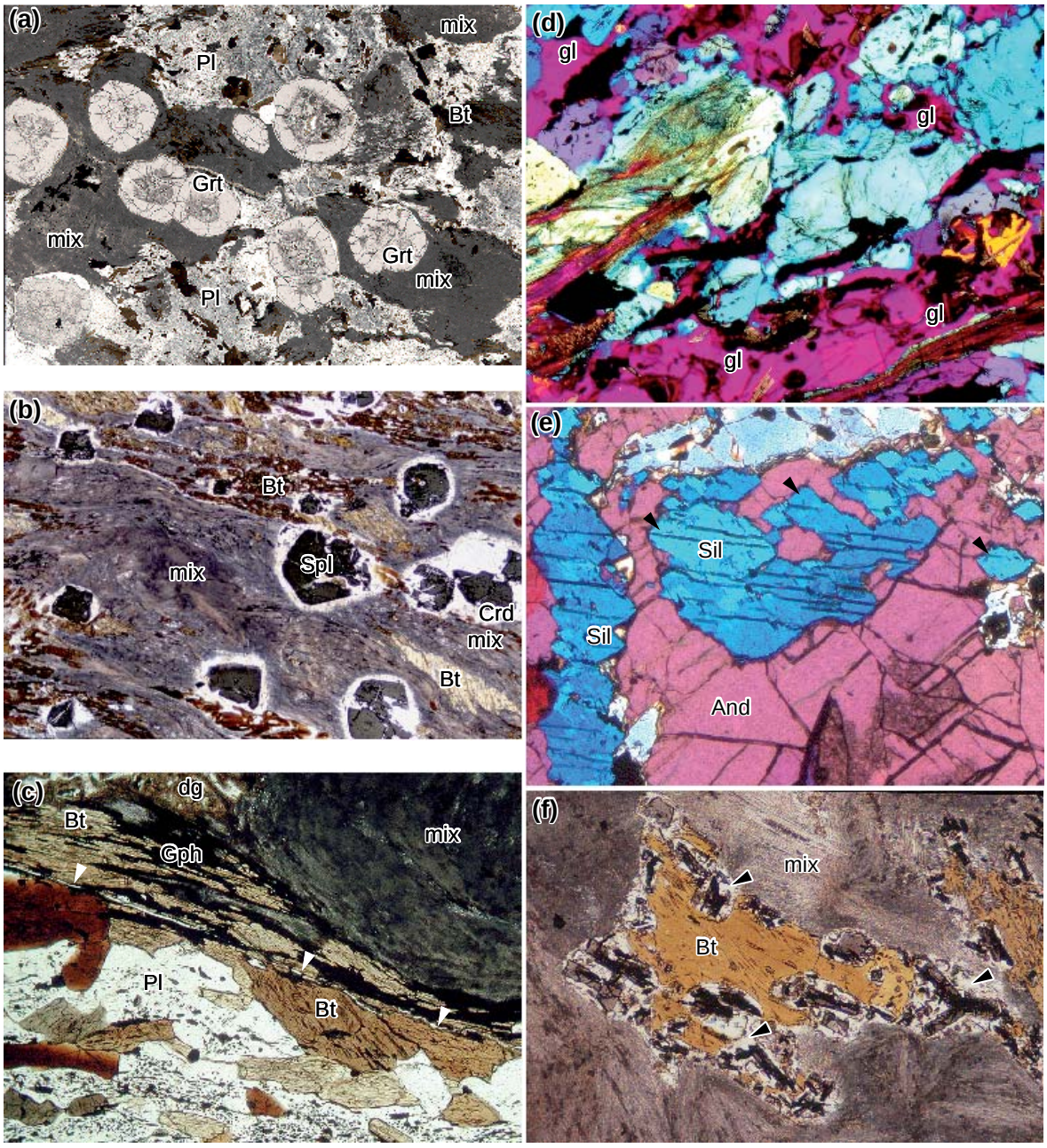

Fig. 3-1. a) Typical Bt-Grt-Sil enclave from El Hoyazo. Note the abundant aggregates of "mix", commonly in contact with euhedral porphyroblasts of garnet. The darker cores of garnet contain abundant inclusions of melt. Plane-polarized light; width of field 30 mm. **b)** Typical Spl-Crd enclave from El Hoyazo. The matrix around spinel is mainly composed of "mix" and biotite, whereas coronae around spinel consist of cordierite or K-feldspar. Plane-polarized light; width of field 5 mm. **c)** Thin film of glass (arrows) along the foliation marked by biotite, graphite and "mix". A patch of devitrified, weathered glass (dg) is visible at the strain shadow around the nodule of mix. Plane-polarized light; width of field 5 mm. **d)** A thick layer of glass (gl, red-violet) in the lower portion of the image is connected to an intergranular network of thinner glass films in the upper portion. In the network, melt coats rounded crystals. Crossed polars with 530 nm accessory plate; width of field 4.2 mm. **e)** Prismatic sillimanite (blue, arrows) topotactically replacing andalusite (pink). Crossed polars with 530 nm accessory plate; width of field 0.8 mm. **f)** Microstructure of biotite melting in the Qtz-free Bt-Grt-Sil enclaves of El Hoyazo. Products of melting include glass (arrows), spinel and ilmenite. Plane-polarized light; width of field 0.7 mm.

WHY ENCLAVES?

Extending to volcanic settings the terminology discussed and defined by Didier & Barbarin (1991) and Didier & Maury (1991), I will distinguish *xenoliths* – extraneous pieces of rocks in magmas (no genetic relations) – from (*cognate*) *enclaves* – fragments showing genetic links to their host rocks. The added value of enclaves, discussed in detail below, is that they bear regional-scale information on the source region of magmas: in the case of metapelitic protoliths, the residual enclaves can be compared with the melanosomes of migmatites and regarded as equivalents.

The uniqueness of enclaves in volcanic rocks for the understanding of crustal melting and the behavior of migmatites can be understood by considering a schematic *T*–*t* diagram such as in Figure 3-2, which shows the different trajectories that rocks undergoing partial melting (either regionally or by contact with magmas) may exhibit. After the peak of metamorphism and anatexis, the cooling of regionally metamorphosed migmatite and granulite terrains (field 1) may take 10^6–10^7 years, and that of enclaves in plutonic rocks (field 2) 10^5–10^6 years. Conversely, that of enclaves in volcanic rocks (path 3) may take 10^{-5}–10^{-1} years (minutes to months): this is the only geological process by which the evidence of melting can be preserved. Figure 3-2 also shows the difference between enclaves and pyrometamorphic xenoliths (path 4). The latter did not share the slow prograde path of the other rocks, and were suddenly heated during entrainment in the host lava (discussion in Holness 2008). It follows that the importance of enclaves in volcanic rocks is given by the combination of extremely rapid cooling and deep crustal provenance. In this perspective, the definition of "*erupted migmatites*" attributed by Zeck (1970) to the enclaves of El Hoyazo in the NVP is most appropriate.

While enclaves (and xenoliths as well) are widespread in mafic volcanic rocks and therefore have become the main subject of study in mantle petrology and geochemistry (*e.g.,* Nixon 1987), the same cannot be said for crustal enclaves in felsic volcanic rocks, especially those that contain partial melts, which are rare and more subject to dissolution during transport (Tsuchiyama 1986). In addition to being rare, crustal enclaves and xenoliths also have other drawbacks, intrinsic to their nature, when compared to migmatites. These are the small size, the lack of outcrop continuity and the lack of precise information on their source, that make it difficult to extrapolate from them on to a regional scale.

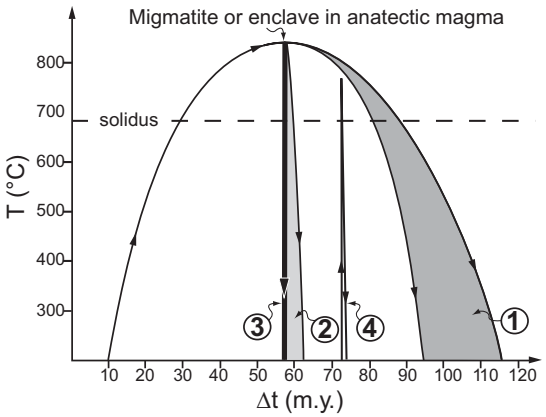

FIG. 3-2. Schematic temperature (*T*) – time elapsed (Δ*t*) diagram with model trajectories of migmatite and granulite (field 1), of enclaves and xenoliths in intrusive rocks (field 2), of enclaves in volcanic rocks (path 3) and of pyrometamorphosed xenoliths (path 4). See text for discussion.

The genetic relationship of rock fragments to host magma is a very important issue, especially in connection with the possibility of retrieving information about the source regions of granite. It is obvious that if the enclaves we observe are the residues of melting (restite) that are genetically linked to a specific magmatic rock, then we can learn a lot more about the regional process of anatexis.

Vernon (2007) has discussed in detail the problem of identifying restite in S–type magmas, concluding that microstructural and isotopic evidence is either against restite or is ambiguous. Among the case studies in support of Vernon's analysis are the enclaves of El Hoyazo that are the subject of this chapter, for which we propose a residual (restite) origin (Cesare *et al.* 1997, Cesare *et al.* 2003a, Perini *et al.*, in press).

I believe that *demonstrating* the residual (restitic) nature of enclaves in volcanic rocks is probably an impossible goal, since we are distant in time and space from the locus where the melting occurred. Therefore, data can only *support* a restite origin that should be generally evaluated and discussed in terms of likelihood and consistency, rather than proof. Except for the origin of melt inclusions in garnet (discussed below), I am not going into the details of the restite problem applied to the enclaves of El Hoyazo, because it is beyond the scope of this chapter. I would only reaffirm that when currently available data from these rocks are considered, they are consistent with restite.

MELT (AT LAST!)

As outlined above, the uniqueness of enclaves (and xenoliths) in volcanic rocks is the preservation of melt, quenched by rapid cooling, in the form of glass. This is the only situation where one can actually talk about "melt", whereas in most other occurrences the term melt is used for its crystallization products or for single mineral phases pseudomorphing the microstructural sites of former melt (*e.g.*, Holness 2008). In the NVP lavas, fresh, undevitrified glass occurs throughout the enclaves in various microstructural domains.

Intergranular films

Glass is commonly present in films and layers of variable thickness, orientation and aspect ratio depending on the mineralogy of, and the degree of melt extraction from, the rock. In strongly foliated, residual (feldspar-poor) samples, glass films are some tens of micrometres thick (Fig. 3-3) and often oriented parallel to the foliation defined by the preferred orientation of biotite, sillimanite and graphite (Fig. 3-1c). Films of glass may also coat the porphyroblasts of garnet (Fig. 3-4), and in all cases there is no mineralogical control on the location of glass films, *i.e.,* glass is not located between reactant minerals. Although some glass fills thin veinlets at a high angle to the foliation (Fig. 3-5), the preferential location of glass films parallel to the layering supports the observations of Guernina & Sawyer (2003) and suggests a control by externally imposed stresses.

In less foliated, more feldspathic enclaves, glass films are thicker (>100 μm) and may form an interconnected network around rounded crystals (Fig. 3-1d).

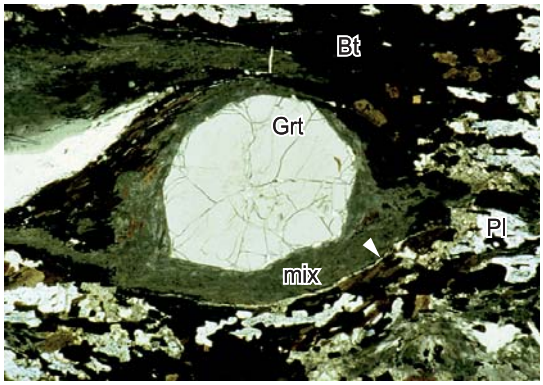

FIG. 3-3. Thin film of glass (arrows) parallel to the foliation that is deflected around a porphyroblast of garnet. Garnet shows euhedral crystal faces toward "mix". Plane-polarized light; width of field 12 mm.

A less common occurrence of glass films is at boundaries between reacting phases, in particular biotite and sillimanite (Cesare 2000, Ferri *et al.* 2007). These microstructures, described in detail below, develop in a static regime, and the glass film (>50 μm) also contains the other products of a melting reaction (*e.g.*, spinel, ilmenite, orthopyroxene).

Glass pockets

Locally, glass is present in large (>500 μm across) pockets located at strain shadows around

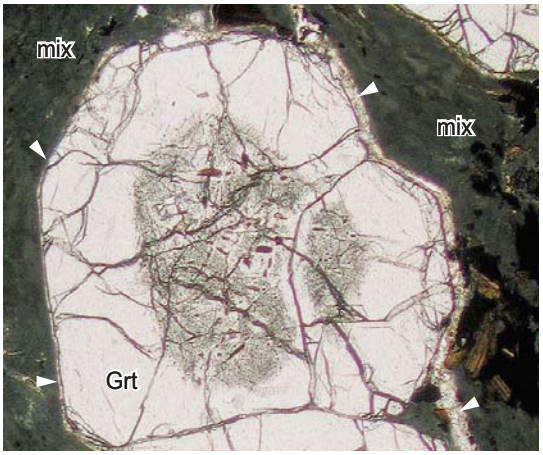

FIG. 3-4. Garnet porphyroblast, with core containing many inclusions of melt and biotite, coated by a thin film of glass (arrows). Garnet shows euhedral crystal faces toward "mix". Plane-polarized light; width of field 5 mm.

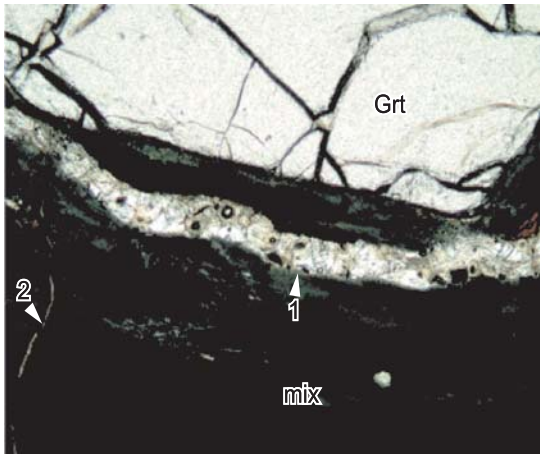

FIG. 3-5. Close-up of a Grt-"mix" boundary from the same sample as in previous figure, showing a thick (*ca*. 100 μm), foliation-parallel layer of partly devitrified glass (1) and a much thinner (<10 μm) glass veinlet quasi-orthogonal to the foliation (2). Plane-polarized light; width of field 1.5 mm.

garnet (Fig. 3-6). This microstructure is mostly observed in the intensely foliated Bt–Grt–Sil enclaves that contain garnet porphyroblasts up to 1 cm in diameter. Other pockets are observed in statically melted, glass-rich graphitic enclaves, and contain an intergrowth of glass and graphite (Fig. 3-7) indicating C–O–H fluid–melt–rock interactions (*e.g.*, Cesare & Maineri 1999).

"Mix"

The last mode of occurrence of interstitial glass is a peculiar intergrowth with acicular sillimanite (fibrolite according to the definition of Pattison 1992), defined as "mix" by Cesare (2000). The "mix" forms layers elongate parallel to the foliation (see Fig. 3-1b) but also nodular aggregates, up to 1 cm across, with size and spatial distribution similar to that of garnet. In the same thin section, "mix" is observed both at the contact with euhedral garnet porphyroblasts, suggesting textural equilibrium, and as faceted knots that partially or totally pseudomorph the garnet (Fig. 3-8, see also Cesare 2000, Fig. 1). This controversial behavior can be interpreted either as the result of replacement (by "mix") of a chemically unstable garnet in favor of a stable one, or as the result of a kinetically controlled behavior of garnet, with growth or dissolution in the different compositional domains of the rock as modeled by Foster (1986). Backscattered SEM imaging (Fig. 3-9) and chemical analyses (Cesare 2000) provide details of the "mix": it consists of a two-phase combination of sillimanite and a rhyolitic melt in proportions that vary from *ca*. 25 wt.% to *ca*. 40 wt.% melt.

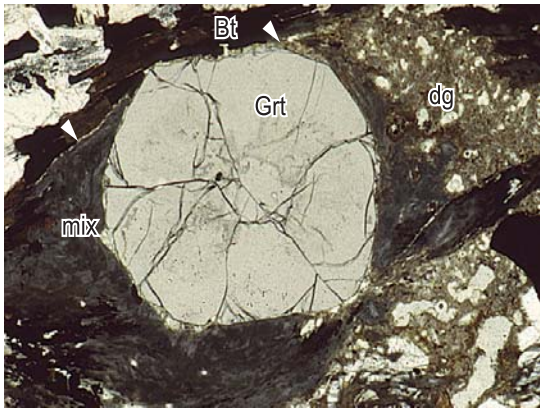

FIG. 3-6. Large pocket of devitrified glass (dg) in the strain shadow of a porphyroblast of garnet. Thin foliation-parallel films of glass are also visible (arrows). Plane-polarized light; width of field 10 mm.

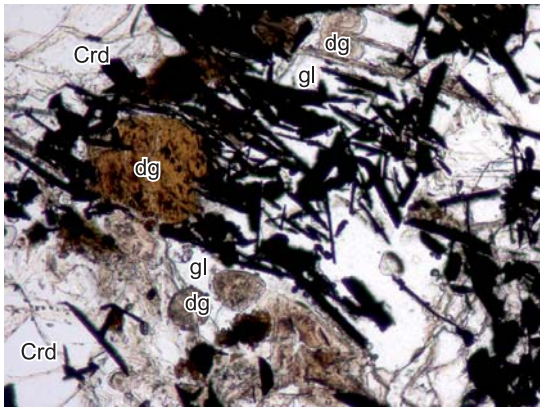

FIG. 3-7. Intergrowth of graphite lamellae (black) and fresh (gl, colorless) or devitrified (dg, brown) glass in a pocket located among cordierite crystals. Plane-polarized light; width of field 2 mm.

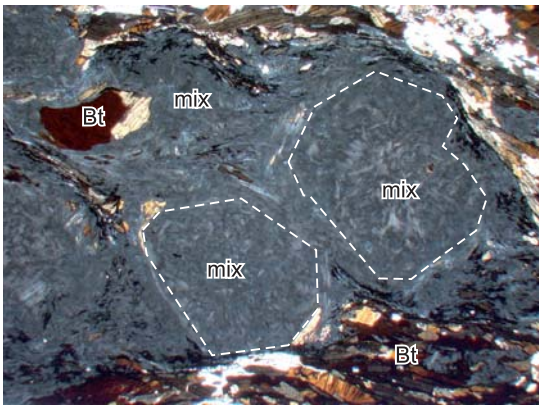

FIG. 3-8. Faceted knots of "mix" which have size and shape compatible with pseudomorphs after garnet, in a Bt-Grt-Sil enclave from El Hoyazo. Plane-polarized light; width of field 8.5 mm.

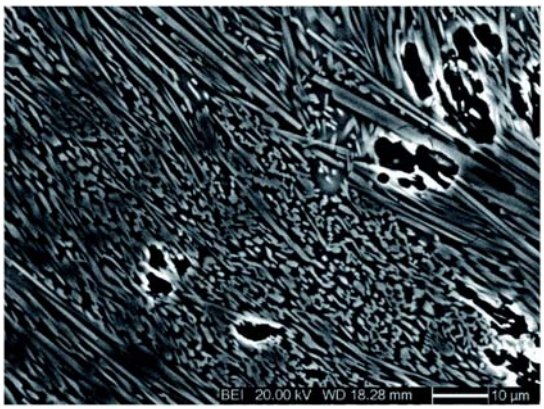

FIG. 3-9. Backscattered SEM image of the "mix" aggregate, consisting of acicular sillimanite (lighter gray) and interstitial glass (darker gray).

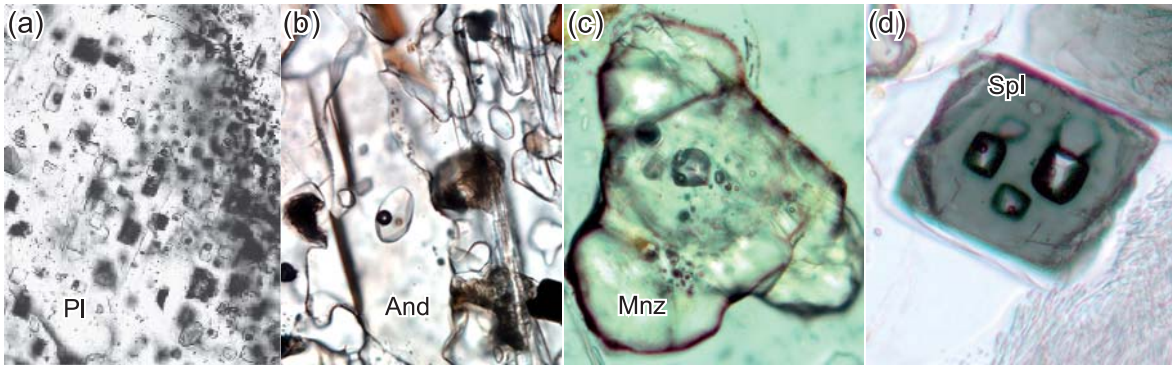

FIG. 3-10. Examples of melt inclusions in various hosts from the enclaves of the NVP. **a)** regular, negative crystal, melt inclusions in plagioclase. Plane-polarized light; width of field 0.5 mm. **b)** isolated melt inclusion in andalusite from Mazarrón. Plane-polarized light; width of field 0.3 mm. **c)** one large and many small melt inclusions in monazite. Plane-polarized light; width of field 200 μm. **d)** negative crystal melt inclusions in spinel. Plane-polarized light; width of field 200 μm.

Dealing with rock fragments that underwent rapid decompression, one question to be asked is if the interstitial glass forming the films, pockets and "mix" described above could result from the impregnation of microfractures by melt from the host lava, rather than being the anatectic melt in equilibrium with the solid assemblage at depth? Although infiltration in a fracture network formed during decompression is commonly observed in mantle xenoliths (*e.g.*, Faure *et al.* 2001), this phenomenon can be ruled out in the enclaves from El Hoyazo, since the composition of the intergranular glass in the enclaves is markedly different to that of the host dacite (Cesare *et al.* 1997).

Melt inclusions

Even if they actually contain glass (quenched melt), the term "melt inclusion" is generally preferred and used (*e.g.*, Webster 2006), and I will adopt it here. Probably the most relevant feature of the enclaves of the NVP is that melt inclusions are present and abundant in all the types of enclave, and in virtually all the minerals, including plagioclase, garnet, cordierite, biotite, spinel, ilmenite, andalusite, corundum, quartz, apatite, zircon and monazite (Fig. 3-10, see also Cesare *et al.* 1997, 2003b, 2003c, 2007, Cesare & Maineri 1999, Álvarez-Valero *et al.* 2005, 2007, Acosta-Vigil *et al.* 2007). For some mineral hosts (*e.g.*, andalusite, cordierite, zircon) this is the first ever occurrence of melt inclusions to be reported (source: Fluid Inclusion Research, volumes 1–31). In general melt inclusions have a maximum size that rarely exceeds 50 μm (up to 100 μm in plagioclase or cordierite) and contain clear, undevitrified glass, commonly with one or more shrinkage bubbles (Fig. 3-11). This has allowed the chemical composition of glasses in inclusions to be analyzed by *in situ* techniques such as EMP and LA–ICP–MS (*e.g.*, Cesare *et al.* 2003a). The shape of the inclusions ranges from spherical to irregular to a faceted negative crystal, and is a function of the type of host mineral and of the time that the enclaves resided at high temperature. In places, as described in detail by Acosta-Vigil *et al.* (2007) the presence of daughter crystals of the host (*e.g.*, ilmenite, plagioclase) or of other phases (*e.g.*, alkali feldspar in plagioclase) indicates post-entrapment crystallization of the melt or interaction between the melt and its host. The zonal arrangement (Sobolev & Kostyuk 1975, Bodnar & Student 2006) of melt inclusions within their hosts is particularly evident in garnet (Fig. 3-12), where inclusions are typically concentrated at the core of crystals. This is consistent with a primary origin (Roedder 1984), *i.e.*, with entrapment of glass droplets by the host mineral during its growth.

A primary origin for the melt inclusions is crucial in determining the petrogenetic significance of enclaves: in fact, it in turn implies that the host mineral has grown in the presence of melt and therefore attests to a partial melting event of peritectic nature (*i.e.*, an incongruent melting reaction). Since this interpretation has recently been challenged by Vernon (2007), I will discuss this issue in detail below.

ORIGIN AND SIGNIFICANCE OF GLASS INCLUSIONS IN CRUSTAL ENCLAVES

The process proposed by Vernon (2007) for the origin of melt inclusions in garnet crystals from

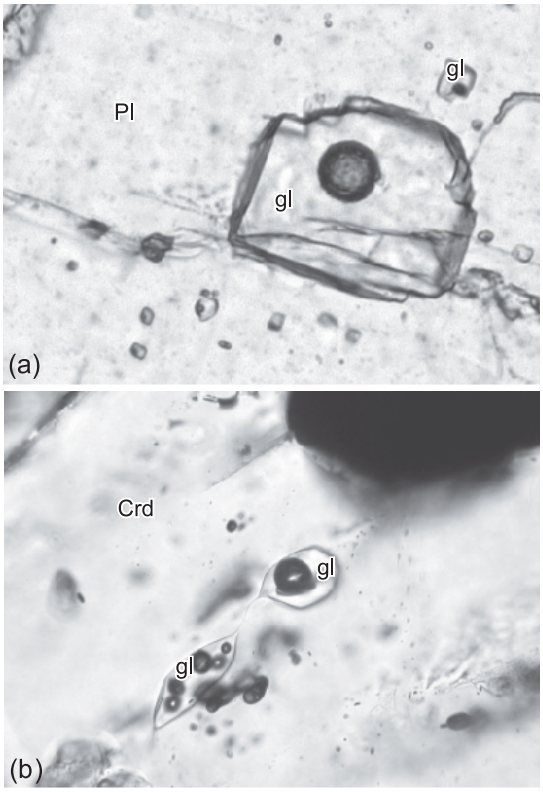

FIG. 3-11. Examples of melt inclusions containing clear and undevitrified glass (gl). **a)** negative crystal-shaped melt inclusions in plagioclase. Plane-polarized light; width of field 180 μm. **b)** irregular inclusion in cordierite, showing many shrinkage bubbles and "necking down" (Roedder, 1984). Plane-polarized light; width of field 120 μm.

the enclaves of El Hoyazo is "melting in response to loss of stability of a mineral assemblage" that "may conceivably produce melt droplets dispersed all through the grains of the unstable mineral if inclusions were originally present, which is a common situation in metamorphic assemblages". Continuing that "instability of inclusion-rich cores during the melting, rather than incorporation of melt droplets during growth" is suggested, he concluded that "glass inclusions must have formed later" than garnet. In essence the mechanism proposed (hereafter termed "*inclusion melting*") is the melting of mineral inclusions contained within an already present garnet. This model, while not unfeasible, is subject to severe constraints, keeping in mind that (for further details see Acosta-Vigil *et al.* 2007): i) melt inclusions in garnet from El Hoyazo are composed of undevitrified glass (see Fig. 3-12b), an empty shrinkage bubble and, in a few cases, include graphite or heavy element(s)-bearing minerals as

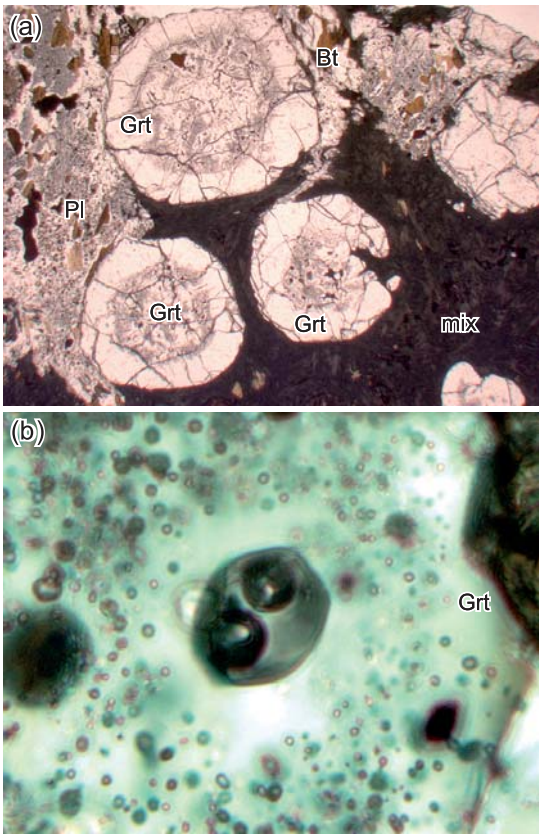

FIG. 3-12. Representative features of melt inclusions in garnet from Bt-Grt-Sil enclaves from El Hoyazo. **a)** zonal arrangement of inclusions at the core of garnet porphyroblasts. Plane-polarized light; width of field 8.5 mm. **b)** enlargement of inclusion-rich zone in garnet, showing that inclusions are composed of clear glass and shrinkage bubble(s), and are optically free of solid phases. Plane-polarized light; width of field 80 μm.

the only other mineral phases over hundreds of inclusions observed; ii) inclusions are composed of a leucogranitic peraluminous glass containing significant amounts of Na, K, Ca, Ti, P; and iii) other mineral inclusions in garnet, separate from melt inclusions, are rare and consist of graphite, ilmenite, biotite and sillimanite.

Considering the mass-balance and microstructural constraints on the theoretical behavior of a mineral inclusion (I) in a mineral host (H, in our case garnet), and its melting to produce a melt (M) and possible peritectic phases (P), the possibilities are: eutectic melting (I + H = M) and peritectic (incongruent) melting (I + H = M + P). Eutectic melting produces a M that, compositionally, must lie between I and H. There are no known minerals that may form a eutectic granitic

composition, such as the suite of inclusions observed in garnet, in combination with garnet. Therefore this possibility can be ruled out. Peritectic (incongruent) melting would produce, along with M, significant and detectable amounts of solids within the inclusion. Depending on the nature of I, these P phases could include spinel, ilmenite, sillimanite, corundum and orthopyroxene. Again, this possibility seems inapplicable to those melt inclusions in the garnet crystals from El Hoyazo because, when examined optically, or on backscattered electron images, they do not contain any solid minerals that could be the peritectic phases.

In addition to the mass-balance and microstructural constraints, further constraints are imposed by thermodynamics. The I + H system is chemically pretty simple, but it is rather unusual. Possible inclusions of I phases in the garnet from metapelitic rocks might be biotite, muscovite, quartz, plagioclase and sillimanite. Apart from the unavoidable constraint of there being necessary peritectic products, most of these binaries would have extremely high melting temperatures, or would not melt at all. For example, muscovite inclusions in garnet would not melt at P <10 kbar, T <850°C (Holland & Powell 2001).

Based on the above observations, the *only* way by which "inclusion melting" could take place is that H, rather than a single mineral, includes an *aggregate* of reactant I phases that always happen to occur in exactly the right modal proportions to enable the reaction to be complete congruent melting. Examples would be aggregates of Kfs + Sil + Qtz or Qtz + Pl + Kfs: if in the right modal proportions, these could melt without leaving peritectic (P) phases in the residue (Johannes & Holtz 1996). Note, however that these assemblages are very rare (they are restricted to subsets of the CKNASH system) and also require the presence of an aqueous fluid phase (H_2O) in order to melt at a geologically reasonable temperature (<1000°C, Johannes & Holtz 1996). Theoretically, melting could even occur at low, "minimum melt" temperatures if the inclusion contained the six phases Ms–Ab–Bt–Kfs–Qtz–H_2O (Thompson 1982) in the correct proportions.

At El Hoyazo, where thousands of fresh, P-free melt inclusions are observed within each garnet (and Pl, Hc, Ilm, Crd, *etc.*, as well), where preserved I are single crystals of either Bt, Sil, Ilm, Gph, Zrn, Ap or Mnz, and where glass compositions have a very narrow compositional range (Acosta-Vigil *et al.* 2007), "inclusion melting" would work only if for *each* melt inclusion there was originally an aggregate of solids and H_2O, *each* with exactly the *same* proportions of reactant phases.

Based on the above considerations, I conclude that although Vernon's (2007) model cannot be ruled out, the requirements for it to have operated are so geologically unreasonable, that it is extremely unlikely to be the correct explanation. Furthermore, I believe that this conclusion can be generalized beyond the El Hoyazo example to include all melt inclusions in crustal rocks. Further details on how melt inclusions are trapped during the growth of garnet and plagioclase hosts are provided by Acosta-Vigil *et al.* (2007).

PRESERVATION OF HIGH TEMPERATURE ASSEMBLAGES

In keeping with the products of experimental quenching, enclaves have the great advantage of not being affected by late stage retrogression and re-equilibration upon cooling. This implies that the phase assemblages and the phase compositions are the same as, or the closest possible to, those that existed at the time of anatexis. Since the dimensions of the crystals and the glass inclusions are big enough to enable several analytical techniques to be used, all the phases in the enclaves have been subjected to an extensive chemical characterization, and this has allowed a better understanding of the mineralogy of high temperature (HT) metapelitic systems.

Chemistry and crystallography of minerals

Table 3-1 reports the representative composition of minerals and of the bulk rock in a typical Bt–Grt–Sil enclave from El Hoyazo and can be considered representative of this enclave type (see also Cesare *et al.* 1997, 2003a, 2005).

Biotite has provided important information that is commonly erased by retrograde processes in migmatites and granulites (*e.g.*, Cesare *et al.* 2008) on the relationships between H and Ti contents in high temperature metapelitic rocks. By integrating EMP data with the direct measurement of H by SIMS and Fe^{3+} by Mossbauer spectrometry, Cesare *et al.* (2003b) have demonstrated the importance of dehydroxylation and Ti-oxy exchange [$(Fe, Mg)^{2+}$ + 2(OH) = Ti + 2O]. Along with its implications on the thermodynamic model of biotite (recently updated by White *et al.* 2007) the Ti-oxy exchange

TABLE 3-1. Representative composition of mineral phases and bulk rock in a typical Bt-Grt-Sil enclave (Ssmple HO50) from El Hoyazo.

Phase	Bt	Grt	Crd	Pl	Kfs	Sil	Ilm	melt	bulk rock
SiO_2	34.43	36.97	48.19	61.19	64.93	36.52	0.04	72.68	47.71
TiO_2	4.86	0.01	0.00	0.02	0.01	0.00	53.34	0.09	1.37
Al_2O_3	18.84	20.55	32.29	24.38	18.79	61.83	0.18	13.16	26.84
Cr_2O_3	0.06	0.02	0.02	0.01	0.00	0.01	0.03	0.02	n.a.
FeO	23.44	37.00	11.74	0.01	0.06	0.20	45.56	0.74	9.83
MnO	0.04	1.28	0.10	0.00	0.02	0.00	0.29	0.01	0.12
MgO	6.35	3.46	6.64	0.00	0.00	0.05	0.89	0.11	2.16
CaO	0.01	1.03	0.01	6.01	0.17	0.06	0.02	0.30	2.58
Na_2O	0.41	0.00	0.11	7.35	2.32	0.01	n.a.	1.72	2.91
K_2O	8.55	0.01	0.10	0.82	12.03	0.04	n.a.	5.58	2.97
L.O.I.	--	--	--	--	--	--	--	--	2.67
Total	96.99	100.34	99.20	99.80	98.32	98.72	100.34	94.40	99.14

has important consequences on high temperature petrogenesis, the most important being a major decrease (30–40%) in the availability of H_2O to the system, which in turn affects the estimates of melt productivity and the mass balance calculations of all Bt-bearing reactions during crustal melting (discussion in Cesare *et al.* 2003a).

Plagioclase in the Bt–Grt–Sil enclaves is homogeneous, with a relatively sodic ($An_{27–33}$) composition, which might seem incompatible with the high inferred equilibration temperatures (850 ±50°C). Note, however, that similar compositions are reported in experimental studies of partial melting of metagreywacke and semipelitic bulk compositions in the range 800–900°C (*e.g.*, Montel & Vielzeuf 1997, Nair & Chacko 2002), and that also in regional migmatites a sodic composition of plagioclase turns out to be present both in the melt-derived fraction and in the residuum (*e.g.*, Gupta & Johannes 1982, Kenah & Hollister 1983).

Graphite is extremely abundant in the enclaves, which may contain up to 1.2 wt.% carbon (Ferri *et al.* 2007). The degree of ordering (crystallinity) of the different textural generations of graphite has been determined by Raman spectroscopy (Cesare & Maineri 1999), who found that the highest state of ordering was in the fine-grained crystals associated with the melt inclusions in plagioclase (Fig. 3-13) and the lowest was in the coarse lamellae and aggregates in the rock matrix. These variations have been interpreted to be related to the progressive graphitization of the sedimentary carbonaceous matter (French 1964, Beyssac *et al.* 2002), and as the evidence for the syn-anatectic precipitation of highly crystalline graphite during fluid-present melting (Cesare & Maineri 1999).

Other minerals, not occurring in the Bt–Grt–Sil enclaves, are worthy of mention.

Spinel is hercynite-rich (X_{Mg} = 0.13–0.22) and Zn-poor, and very common in the Spl–Crd enclaves of El Hoyazo and also at the Mazarrón and Mar Menor localities. It commonly forms euhedral mm-sized crystals, and it is these that have had their intracrystalline cation ordering studied by single crystal X-ray diffraction. Interestingly, these Mg-hercynite crystals display the largest disordering observed in natural spinel, with cation ordering

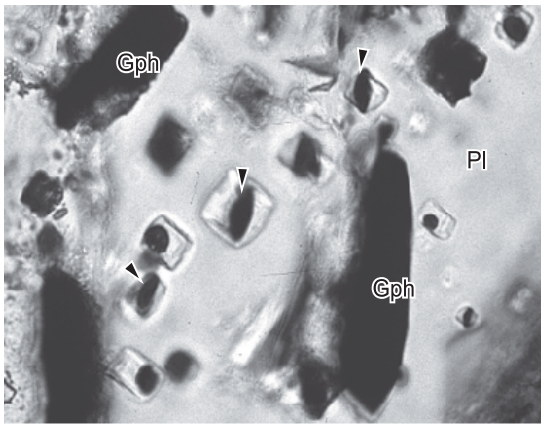

FIG. 3-13. Graphite (black) and melt inclusions in plagioclase. Tiny graphite crystals occur sparsely within some melt inclusions (arrows). These graphite lamellae represent solid inclusions and not daughter crystals and exhibit the highest crystalline ordering. Plane-polarized light; width of field 130 μm.

closure temperatures in the range 700–900°C (Lavina, pers. comm., 2008). These data indicate that in rapidly cooled rocks, intracrystalline cation ordering in spinel may provide additional constraints to thermometry.

Al_2SiO_5 polymorphs are also common in the enclaves: fibrolite dominates, whereas prismatic sillimanite is much rarer. Andalusite is common at Mazarrón and Mar Menor, and in the former locality it is commonly pseudomorphed by prismatic sillimanite (Fig. 3-1e). The direct topotactic (crystallographically controlled) transformation of andalusite to sillimanite was characterized by TEM in samples from Mazarrón (Cesare *et al.* 2002), where it was observed that the two lattices are rotated by ~2.5° around a_{And} (= b_{Sil}) with respect to the topotactic relationship previously proposed in the literature ($c_{And} \parallel c_{Sil}$, $a_{And} \parallel b_{Sil}$, $b_{And} \parallel a_{Sil}$, Vernon 1987). In addition, the finding of microscopic lamellae of sillimanite within seemingly homogeneous andalusite has important implications for the interpretation of phase equilibria in aluminous metapelite, as it suggests that many "andalusite-grade" rocks might in fact contain optically undetectable sillimanite, and that a correct assessment of the And–Sil transition should be rigorously performed by TEM investigation.

Chemistry of melts

As outlined before, the enclaves of the NVP offer the unique possibility of determining the composition of natural anatectic melts, both those occurring as intergranular films and, especially, those trapped as melt inclusions in the various mineral hosts. After some preliminary characterization (Cesare *et al.* 1997, 2003c, 2005, Cesare 2000, Cesare & Gómez-Pugnaire 2001), the systematic study of the composition of glasses in the Bt–Grt–Sil enclaves of El Hoyazo has been undertaken by Acosta-Vigil *et al.* (2007), who obtained the first dataset of anatectic melts from natural pelitic rocks. Unlike the case of rapidly melted xenoliths in lavas (*e.g.*, Braun & Kriegsman 2001, Salvioli Mariani *et al.* 2005), where glasses exhibit very large compositional ranges, the melts in the enclaves we studied are remarkably homogeneous in composition. They are granitic, peraluminous and felsic (leucogranite), with a moderate Aluminum Saturation Index (Table 3-2). Interestingly, there are systematic differences in the glass compositions from different textural settings in the enclaves, but all glasses from a specific textural location (i.e., within a specific host mineral) all have comparable compositions. These relationships are maintained between different enclaves in an outcrop, and have been interpreted as recording the evolution of the composition of the melt during prograde anatexis of the quartz-poor metapelite. Because H_2O concentrations are below the saturation levels for granitic melts at the inferred pressures of melting (*e.g.*, Holtz *et al.* 1995), Acosta-Vigil *et al.* (2007) concluded that crustal anatexis occurred under H_2O-undersaturated

TABLE 3-2: Representative compositions of glasses in the enclaves of the NVP.

Host	Plagioclase	Garnet	Cordierite	Ilmenite	Andalusite	Interstitial
Source	1	1	1	1	2	3
SiO_2	73.28	71.26	73.42	70.68	71.21	70.47
TiO_2	0.08	0.10	0.07	0.31	0.09	0.21
Al_2O_3	12.64	14.44	14.01	15.69	13.87	15.10
FeO_{tot}	1.15	1.72	1.31	2.58	1.46	1.13
MnO	0.02	0.08	0.04	0.07	0.15	0.03
MgO	0.15	0.05	0.04	0.13	0.12	0.13
CaO	0.24	0.60	0.93	0.96	0.61	1.03
Na_2O	2.85	3.61	3.41	3.55	2.72	3.57
K_2O	5.00	4.97	4.92	4.92	5.74	5.76
P_2O_5	0.21	0.37	0.20	0.31	n.a.	n.a.
F	0.06	0.08	0.05	0.07	n.a.	n.a.
Cl	0.04	0.01	0.45	0.01	0.27	n.a.
Total	95.72	97.29	98.85	99.28	96.15	97.43

All data refer to melt inclusions (hosted by mineral listed in first row) except for the rightmost column of interstitial glass rimming biotite melting to hercynite. Sources of data: 1) Acosta-Vigil *et al*. (2007); 2) Cesare et al. (2003c); 3) Cesare (2000).

conditions. In fact, the compositions of the melt in the inclusions compare closely to those of glasses produced by experimental, fluid-absent partial melting of metapelitic rocks (*e.g.*, Le Breton and Thompson 1988, Vielzeuf and Holloway 1988, Patiño Douce & Johnston 1991).

The composition of the glass within the melt inclusions has also been a key to constraining the much-debated location of the Al_2SiO_5 triple point in *P–T* space. Andalusite in the *xenoliths* from Mazarrón (here the genetic link to the host lava is less straightforward) shows the systematic occurrence of large and primary primary melt inclusions (see Fig. 3-10b), and these were analyzed by EMP and LA–ICP–MS (Cesare *et al.* 2003c). Based on the content of the volatile elements, B, Cl and F, and on the occurrence of graphite in these rocks, the displacement of the wet granite solidus in P–T space was calculated, and compared to the location of the And–Sil equilibria from Holdaway (1971) and Pattison (1992). Because an And + melt stability field, as observed in the enclaves, was generated using the And–Sil equilibrium of Pattison (1992), but not with that of Holdaway (1971), the former is preferred and should be used.

While there is little doubt that the composition of glass in the inclusions from the enclaves is that of a partial melt produced by anatexis, the connection with migmatites is less straightforward. In general, leucosome in migmatites is not considered to be primary anatectic melt because of the possible presence of restitic phases and/or cumulus phenomena (*e.g.*, Sawyer 1987, Solar & Brown 2001). Alternative methods should be sought: on the basis of the example of enclaves from the NVP, one might look for former melt inclusions also in migmatites and granulites. Target host minerals should be the peritectic phases (*i.e.*, garnet, orthopyroxene and spinel) that grow during the melting reaction and, therefore, have more potential to trap droplets of melt. In slowly cooled regional anatectic rocks the melt inclusion will have crystallized to an aggregate of different minerals (quartz, feldspars and micas), and this is what should be expected. One example of former melt inclusions in granulite can be observed in Fig. 3-14 (Ferrero, pers. com.). These microcrystalline aggregates within garnet from the "khondalite" of the Kerala Khondalite Belt of SE India are mainly composed of quartz, feldspars and biotite, have been experimentally melted at *ca*. 950 °C, and the homogenized composition can then be analyzed by EMP.

MELTING REACTIONS

In the enclaves, melting reactions are outlined by microstructures that involve intergranular films of glass which are commonly well preserved and can be analyzed, allowing a better chemical characterization of the melt-producing reaction. In many cases the most straightforward microstructures indicate a static event that overprints and postdates the main anatectic assemblage (*e.g.*, Bt–Grt–Sil).

The melting of biotite in the Qtz-free, Bt–Grt–Sil enclaves has been modeled by Cesare (2000) through the study of peculiar reaction rims that are composed of glass, spinel and ilmenite, and which occur at the contact between biotite and "mix" (Fig. 3-1f). After detailed microstructural and microchemical characterization (glass composition reported in Table 3-2), algebraic analysis (Fisher 1989, Cesare 1999) was performed in the nine-component (Al–Ca–Fe–K–Mg–Mn–Na–Si–Ti), nine-phase (Bt_1–Bt_2–Grt–Spl–Ilm–melt–mix–Pl_1–Pl_2) system, and provided the balance:

$$0.78\ Bt_1 + 1.95\ Pl_1 + 2.82\ mix + 0.32\ Grt = 0.25\ Ilm + 5.00\ melt + 0.30\ Bt_2 + 2.53\ Spl + 1.03\ Pl_2 \quad (1)$$

This relationship is in agreement with the observed textures and can, therefore, be considered a good model for the incongruent melting of biotite in the Qtz-free enclaves (Cesare 2000). As this reaction requires garnet and plagioclase as reactants, the reaction volume must be larger than the site at which the melt is produced, where these two phases are not present. Ferri *et al.* (2007) have reproduced the same reaction experimentally in cores of Bt–Grt–Sil enclaves melted at 950°C and 5 kbar.

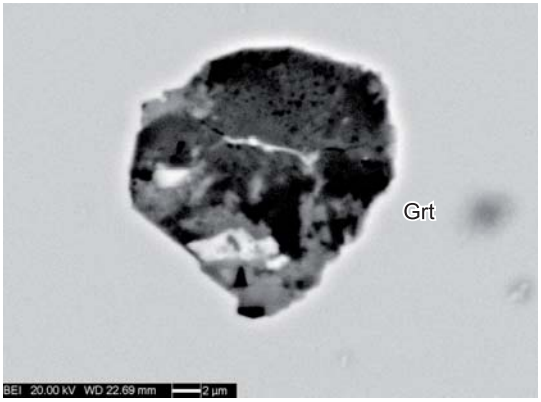

FIG. 3-14. Backscattered SEM image of a polycrystalline inclusion in garnet from a metapelitic granulite ("khondalite") of the Kerala Khondalite Belt, probably representing a former melt inclusion, crystallized during slow cooling (courtesy S. Ferrero).

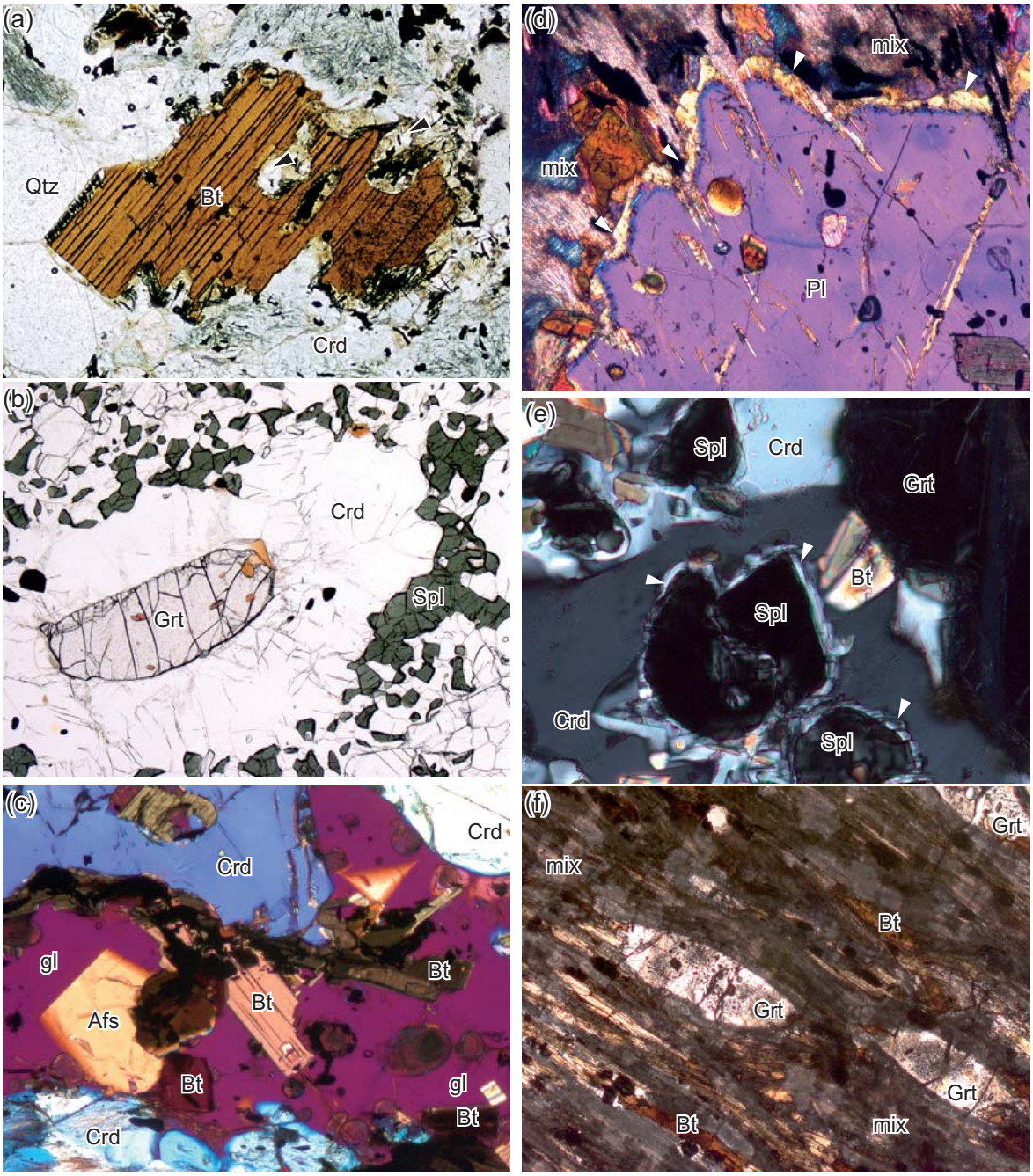

FIG. 3-15. **a)** Microstructure of biotite melting in the Qtz-Crd rocks of El Hoyazo. Products of melting include glass (arrows), orthopyroxene and ilmenite. Note uneven distribution of the reaction rim. Plane-polarized light; width of field 0.6 mm. **b)** Reaction corona of cordierite and spinel in a khondalite from the Kerala Khondalite Belt. Plane-polarized light; width of field 8 mm. **c)** Euhedral crystallites of alkali feldspar (Afs) and biotite in a thick glass layer bounded by embayed cordierite (right). Crossed polars with 530 nm accessory plate; width of field 0.4 mm. **d)** Sodic rim (yellow, arrows) overgrowing a crystal of more calcic plagioclase (purple) at the contact with a "mix". Crossed polars with 530 nm accessory plate; width of field 0.85 mm. **e)** Thin rim of plagioclase (arrows) around spinel in the Crd-bearing coronae around garnet. Crossed polars; width of field 0.3 mm. **f)** "Elliptical garnets" from a highly deformed enclave of El Hoyazo. Plane-polarized light; width of field 3 mm.

A similar reaction microstructure is observed in Qtz-bearing enclaves, namely in the Qtz–Crd rocks (as in the definition of Zeck 1970) of El Hoyazo. Here, biotite shows evidence of instability and decomposition (Fig. 3-15a), and a reaction rim up to 100 μm in thickness and consisting of glass, orthopyroxene and ilmenite (Fig. 3-16) has developed. The reaction proceeds only at the Qtz–Bt grain boundaries, whereas adjacent Bt–Crd interfaces remained stable.

In this example, mass balance calculations in the simplified KFMASH–Ti system indicate that the reaction inferred from textural analysis:

$$\text{Bt} + \text{Qtz} = \text{melt} + \text{Opx} + \text{Ilm} \qquad (2)$$

similar to those produced experimentally, for example in the H_2O-saturated melting of Ms + Qtz (Rubie & Brearley 1990).

A third example of microstructures formed by a melting reaction is observed both at El Hoyazo and Mazarrón, and consists of spinel + cordierite + K-feldspar + plagioclase + glass coronae around garnet (Fig. 3-17). These microstructures indicate the breakdown of garnet during decompression and slight heating, and have been characterized by Álvarez-Valero *et al.* (2007). Also in this case the reaction corona developed statically and glass is present between the product phases. However, unlike in the previous examples, the glass occurs mostly as melt inclusions in spinel and cordierite, and only rarely forms an intergranular film. Once again, the full microchemical characterization of phases (including the glass) in the rock has enabled an algebraic analysis of the development of the corona. Although the microstructures are suggestive of a model reaction such as

$$\text{Grt} + \text{Sil}\ (+\text{Pl}) = \text{Spl} + \text{Crd} + \text{Kfs} + \text{melt}, \qquad (3)$$

matrix analysis in the NCKFMASH system indicates the (unbalanced) reaction

$$\text{Grt} + \text{Sil} + \text{Bt} + \text{Pl}_1 = \text{Spl} + \text{Crd} + \text{Pl}_2 + \text{Kfs} + \text{melt} \qquad (4)$$

as the preferred model for the melting reaction (Álvarez-Valero *et al.* 2007).

Although this approach does not always lead to unequivocal results and interpretations, the modeling of melting reactions in enclaves and xenoliths represents a significant improvement, because analyzed, rather than assumed, melt compositions can be considered. Therefore, it has important implications for the petrogenesis of migmatites and granulites, where similar microstructures occur commonly (*e.g.,* Fig. 3-15b).

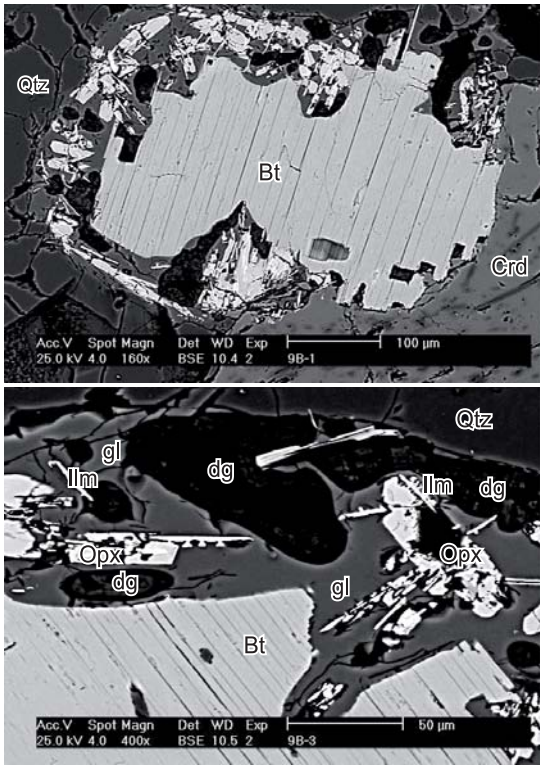

FIG. 3-16. **a)** Backscattered SEM image of a microstructure such as in Fig 3-15a. Note the kinetic control on reaction progress, with extensive reaction at the boundaries with quartz, and little or no reaction at the boundaries with cordierite. **b)** Close-up of a reaction rim around biotite, displaying fresh (gl) and weathered (dg) glass, elongate orthopyroxene and acicular to dendritic ilmenite.

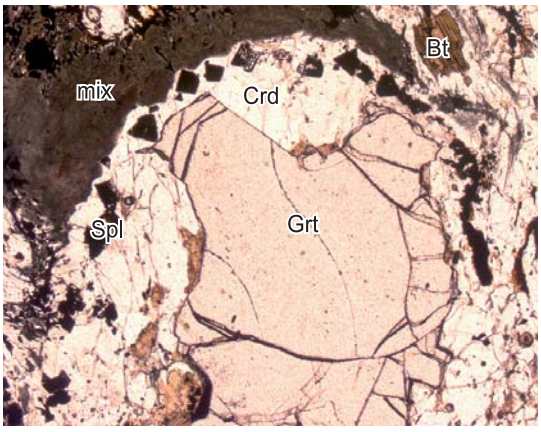

FIG. 3-17. Reaction corona of spinel, cordierite and K-feldspar replacing garnet in an enclave from El Hoyazo. Crossed polars; width of field 8.5 mm.

MELT-CONSUMING (CRYSTALLIZATION) FEATURES

Along with providing insights on the prograde, melt-producing history of high-grade metapelite, the enclaves of the NVP also display local evidence of melt-consuming features, and these can be compared with the microstructures formed during crystallization that are observed in migmatites.

A first example is represented by the small (a few tens of μm) euhedral crystallites of alkali feldspars and biotite that can be observed at the boundaries or within the thickest films of glass in melt-rich enclaves (Fig. 3-15c). These microstructures are comparable to the euhedral crystals rimmed by pseudomorphic quartz and K-feldspar after melt films (*e.g.*, Vernon 2004, Holness 2008– this volume, Figure 4-10), of which they represent the very initial stage of development. Depending on which minerals occur at the boundary with the glass film, the crystallization product may form overgrowths rather than single crystallites, highlighting a kinetic control on nucleation. This is observed when plagioclase is involved: in this case an overgrowth of different composition (alkali feldspar or more albitic plagioclase) projects topotactically towards the "mix" or glass layer (Fig. 3-15d).

Another melt-consuming feature is represented by symplectic intergrowths of biotite–plagioclase or biotite–K-feldspar. The former type is observed as partial pseudomorphs after garnet (Fig. 3-18, see also Figure 2f in Álvarez-Valero *et al.* 2007) and has been interpreted as evidence of a slight cooling event, with partial crystallization, before the eruption of the lavas that host the enclaves.

A similar genetic interpretation has been proposed for the thin rims of plagioclase around spinel (Fig. 3-15e) in the coronae after garnet from the same rocks (Álvarez-Valero *et al.* 2007). These rims represent partial to total "pseudomorphs" after melt, and they are very similar to the microstructures observed in migmatites and granulite discussed by Holness (2008).

INFORMATION ON DYNAMICS

One of the most important features of the enclaves of the NVP is that they show evidence of having been deformed during melting. The syn-anatectic origin of the foliation and other deformation features in the enclaves has been questioned by Vernon (2007) on the basis of his interpretation of melt inclusions in garnet. Since, as outlined above, the "inclusion melting" process proposed by Vernon (2007) is untenable, we can confidently conclude that garnet has indeed grown during melting, and reaffirm the microstructural evidence of syntectonic melting described by Cesare *et al.* (1997), Cesare and Gómez-Pugnaire (2001) and Álvarez-Valero *et al.* (2005).

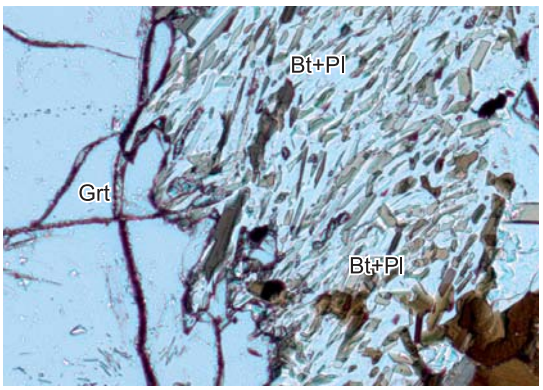

FIG. 3-18. Fine-grained aggregate of biotite and plagioclase partially replacing garnet. Plane-polarized light; width of field 1.5 mm.

A first evidence of the syn-anatectic origin of the main foliation of most enclaves is that it anastomoses around porphyroblasts that contain primary melt inclusions. This is observed both around porphyroblasts of garnet at El Hoyazo and around porphyroblasts of plagioclase at Mazarrón (Cesare & Gómez-Pugnaire 2001). A spectacular example comes from the Bt–Grt–Sil enclaves from El Hoyazo, where the foliation that anastomoses around garnet is marked by the helicitic arrangement of melt inclusions in plagioclase (Fig. 3-19), rather than biotite–sillimanite–glass folia as is generally observed. This microstructure implies the growth of garnet in the presence of melt, and the subsequent deflection of the foliation around it. Growth of plagioclase seems to postdate development of the foliation, but might also be coeval with it. Regardless of the actual timing of the growth of plagioclase, the helicitic foliation included in it and outlined by melt inclusions, attests to a prolonged history of crystallization and deformation in the presence of a melt phase, *i.e.*, during anatexis.

In some cases, melting was accompanied by intense deformation and pressure-solution phenomena. One example is provided by the elliptical garnets (Fig. 3-15f) studied by Álvarez-Valero *et al.* (2005), which show evidence of truncation of the internal pattern of melt inclusions at high strain

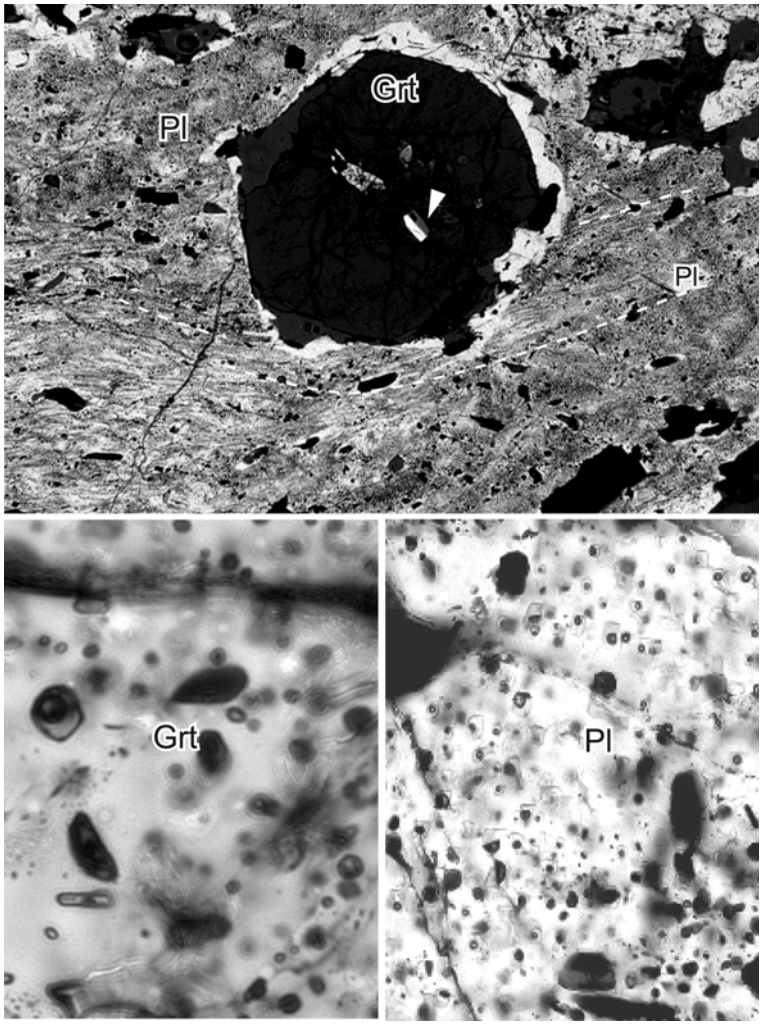

FIG. 3-19. **a)** Porphyroblast of garnet with melt inclusions (enlarged in **b)**) surrounded and enclosed by plagioclase. The garnet includes a Carlsbad-twinned plagioclase (arrow). The plagioclase contains an internal foliation deflecting around garnet, outlined by graphite and melt inclusions (enlarged in **c)**). Crossed polars; width of field 20 mm.
b) close-up of garnet core containing many melt inclusions. Plane-polarized light; width of field 80 μm.
c) close-up of plagioclase containing many melt inclusions and graphite (black). Plane-polarized light; width of field 0.2 mm.

zones, and the redeposition of new garnet and biotite at the strain shadows. Dissolution was probably promoted by the movement of melt away from high-strain zones in the direction along the foliation planes which anastomose around the crystals of garnet. A similar example is observed in quartzofeldspathic enclaves from El Hoyazo, where intensely foliated domains consisting mainly of fibrolitic sillimanite and melt, alternate with layers that have a more granoblastic microstructure (Fig. 3-20a). Also the origin of highly oriented sillimanite folia in these rocks is syn-anatectic, as indicated by the presence of melt inclusions in the lenticular crystals of quartz that are elongate parallel to the foliation (Fig. 3-20b). All the above microstructures demonstrate that the enclaves were not involved in a "static" or contact-melting type of environment, but that melting occurred when the crust was deforming as a coherent body, in a regional-scale process.

The identification of a syn-anatectic deformation in the enclaves demonstrates that the enclaves can provide unique pieces of information about the actual state and dynamic behavior of the partially melted crust. In connection with defining the pathways that the melt followed as it escaped from its residuum, it has been observed that in the most residual, feldspar-poor samples, the intergranular melt is preferentially located on thin, layer-parallel folia, whereas glass-filled fractures oriented at a high angle to the foliation are less common (Figs. 3-1c, 3-5). This supports the conclusion of Cesare *et al.* (1997) that, on a length-scale of up to tens of centimetres, deformation-assisted escape of melt occurred by flow parallel to lithological anisotropies.

It should be noted that the proposition that the deformation recorded by the microstructures in the enclaves occurred before their fragmentation

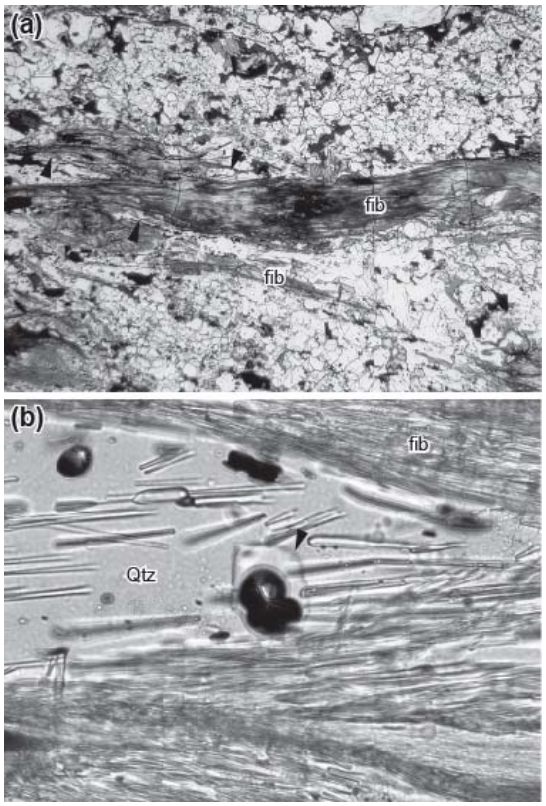

FIG. 3-20. **a)** Quartzofeldspathic enclave with a fibrolite-rich, intensely oriented layer in the central part of the image. Thinner fibrolite folia anastomose in the left-hand side (arrows). Plane-polarized light; width of field 3 mm. **b)** Enlargement of a lenticular quartz crystal wrapped by sillimanite folia. The quartz contains a melt inclusion (arrow). Plane-polarized light; width of field 80 μm.

and inclusion in the lava is not contradicted by the presence of the static microstructures that are present in some of the enclaves that were studied and which have been described above (*e.g.*, biotite-melting reactions and cordierite–spinel coronae after garnet). In fact, the latter microstructures are late with respect to the foliation, and are interpreted as having formed after fragmentation of the metapelite and its entrainment in the lava as enclaves, and during the time which the enclaves were resident in the magma chamber prior to eruption (Álvarez-Valero *et al.* 2007).

CONCLUSIONS

Unfortunately, rocks such as those described in this chapter seem to be very rare in nature, but a careful and focused reinvestigation of outcrops of S-type felsic volcanic rocks is likely to reveal (many) further occurrences. For example, crustal enclaves, xenoliths and xenocrysts with many similarities to those of the NVP occur at Lipari (Eolian islands, Italy; Barker 1989), where garnet and andalusite contain primary melt inclusions (Clarke *et al.* 2005).

Along with the drawback of being rare, enclaves and xenoliths also suffer from the major uncertainty on the location and nature of their source, and from their small size, that may prevent extrapolation of the results obtained from them to regional scale; this may lead one to question their relevance for the overall understanding of anatexis.

Despite these problems intrinsically related to being fragments of rock in "foreign" magmas, the case studies summarized above should suffice to indicate that information from enclaves represents an important complement to field-based studies of migmatite complexes and experimental simulation of crustal melting.

ACKNOWLEDGEMENTS

I wish to thank A. Acosta-Vigil, F. Ferri, and L. Tajcmanova for critically reading this paper, and E. Sawyer for review and for inviting me to take part in this workshop on migmatites. Financial support from Italian MIUR (PRIN 2005-047810) and C.N.R. (Euromargins ESF Eurocore)

REFERENCES

ACOSTA-VIGIL, A., CESARE, B., LONDON, D. & MORGAN, G.B.VI (2007): Microstructures and composition of melt inclusions in a crustal anatectic environment: the metapelitic enclaves within El Hoyazo dacites, SE Spain. *Chem. Geol.* **237**, 450-465.

ÁLVAREZ-VALERO, A.M. & KRIEGSMAN, L.M. (2007): Crustal thinning and mafic underplating beneath the Neogene Volcanic Province (Betic Cordillera, SE Spain): evidence from crustal xenoliths. *Terra Nova* **19**, 266-271.

ÁLVAREZ-VALERO, A.M., CESARE, B. & KRIEGSMAN, L.M. (2005): P-T paths in crustal enclaves: Examples from the Neogene Volcanic Province, Spain. *Geochim. Cosmochim. Acta* **68**, A665-A665 Suppl. S.

ÁLVAREZ-VALERO, A.M., CESARE, B. & KRIEGSMAN, L.M. (2007): Formation of spinel-cordierite-feldspar-glass coronas after garnet in metapelitic xenoliths: Reaction modelling and geodynamic implications. *J. Metamorph. Geol.* **25**, 305-320.

BARKER, D. S. (1987). Rhyolites contaminated with metapelite and gabbro, Lipari, Aeolian Islands, Italy: products of lower crustal fusion or of assimilation plus fractional crystallization? *Contrib. Mineral. Petrol.,* **97**, 460–472.

BODNAR, R.J. & STUDENT, J.J. (2006): Melt inclusions in plutonic rocks: petrography and microthermometry. *In:* Melt Inclusions in Plutonic Rocks (J.D. Webster, *ed.*) Min. Assoc. Can. Short Course **36**, 1-25.

BRAUN, I. & KRIEGSMAN, L.M. (2001): Partial melting in crustal xenoliths and anatectic migmatites: a comparison. *Phys. Chem. Earth, A* **26**, 261-266.

BROWN, M. (2007): Crustal melting and melt extraction, ascent and emplacement in orogens: mechanisms and consequences. *J. Geol. Soc. London* **164**, 709-730.

CESARE, B. (1999) Multi-Stage pseudomorphic replacement of garnet during polymetamorphism: 2. Algebraic analysis of mineral assemblages. *J. Metamorphic Geol*. **17**, 735-746.

CESARE, B. (2000): Incongruent melting of biotite to spinel in a quartz-free restite at El Joyazo (SE Spain): Textures and reaction characterization. *Contrib. Mineral. Petrol.* **139**, 273-284.

CESARE, B. & GÓMEZ-PUGNAIRE, M.T. (2001): Crustal melting in the Alborán domain: constraints from the xenoliths of the Neogene Volcanic Province. *Phys. Chem. Earth, A* **26**, 255-260.

CESARE, B. & MAINERI, C. (1999): Fluid-present anatexis of metapelites at El Joyazo (SE Spain): constraints from raman spectroscopy of graphite. *Contrib. Mineral. Petrol.* **135**, 41-52.

CESARE, B., SALVIOLI MARIANI, E. & VENTURELLI, G. (1997): Crustal anatexis and melt extraction in the restitic xenoliths at El Hoyazo (SE Spain). *Mineral. Mag.* **61**, 15-27.

CESARE, B., GÓMEZ-PUGNAIRE, M.T., SANCHEZ-NAVAS, A. & GROBETY, B. (2002): Andalusite - sillimanite replacement (Mazarrón - SE Spain): microstructural and TEM study. *Am. Mineral.* **87**, 433-444.

CESARE, B., CRUCIANI, G. & RUSSO, U. (2003a): Hydrogen deficiency in Ti-rich biotite from anatectic metapelites (El Joyazo - SE Spain): crystal-chemical aspects and implications for high-temperature petrogenesis. *Am. Mineral.* **88**, 583-595.

CESARE, B., GÓMEZ-PUGNAIRE, M.T. & RUBATTO, D. (2003b): Residence time of S-type anatectic magmas beneath the Neogene Volcanic Province of SE Spain: a zircon and monazite SHRIMP study. *Contrib. Mineral. Petrol.* **146**, 28–43.

CESARE, B., MARCHESI, C., HERMANN, J. & GÓMEZ-PUGNAIRE, M.T. (2003c): Primary melt inclusions in andalusite from anatectic graphitic metapelites: Implications for the position of the Al_2SiO_5 triple point. *Geology* **31**, 573-576.

CESARE, B., MELI, S., NODARI, L. & RUSSO, U. (2005): Fe^{3+} reduction during biotite melting in graphitic metapelites: another origin of CO_2 in granulites. *Contrib. Mineral. Petrol.* **149**, 129-140.

CESARE, B., MAINERI, C., BARON TOALDO, A., PEDRON, D. & ACOSTA-VIGIL, A. (2007): Immiscibility between carbonic fluids and granitic melts during crustal anatexis: a fluid and melt inclusion study in the enclaves of the Neogene Volcanic Province of SE Spain. *Chem. Geol.* **237**, 433-449.

CESARE, B., SATISH-KUMAR, M., CRUCIANI, G., POCKER, S. & NODARI, L. (2008): Formation of glass-bearing spinel-cordierite-feldspars coronas after garnet in metapelitic xenoliths. Reaction modelling and geodynamic implications. *Am. Mineral.* **93**, 327-338.

CLARKE, D.B., DORAIS, M., BARBARIN, B., BARKER, D., CESARE, B., CLARKE, G.L., BAGHDADI, S.E., FÖRSTER, H-J., GAETA, M., GOTTESMAN, B., JAMIESON, R.A., KONTAK, D.J., KOLLER, F., GOMES, C.L., LONDON, D., MORGAN, G.B., NEVES, L., PATTISON, D.R.M., PEREIRA, J., PICHAVANT, M., RAPELA, C.W., RENNO, A.D., RICHARDS, S., ROBERTS, M., ROTTURA, A., SAAVEDRA, J., SIAL, A.N., TOSSELI, A.J., UGIDOS, J.M., UHER, P., VILLASECA, C., VISONA, D., WHITNEY, D.L., WILLIAMSON, B. & WOODWARD, H.H., (2005). Occurrence and origin of andalusite in peraluminous felsic igneous rocks. *J. Petrol.* **46**, 441-472.

CLEMENS, J. D. (2006): Melting of the continental crust: fluid regimes, melting reactions and source-rock fertility. *In*: Evolution and Differentiation of the Continental Crust (M. Brown and T. Rushmer, *eds*.) Cambridge University Press, 297-331.

DIDIER, J. AND BARBARIN B. (1991): The different type of enclaves in granites: Nomenclature. *In*: Enclaves and Granite Petrology (J. Didier & B.

Barbarin, *eds.*), Developments in Petrology **13**, 19-23.

DIDIER, J. & MAURY, R.C. (1991): The outstanding contribution of Alfred Lacroix to the study of enclaves in magmatic rocks. *In*: Enclaves and Granite Petrology (J. Didier & B. Barbarin, *eds.*), Developments in Petrology **13**, 25-32.

DOWNES, H., BEARD, A. & HINTON, R. (2004): Natural experimental charges; an ion-microprobe study of trace element distribution coefficients in glass-rich hornblendite and clinopyroxenite xenoliths. *In*: Trace Element Fingerprinting: Laboratory Studies and Petrogenetic Processes (S.Y. O'Reilly & R. Vannucci, *eds.*) Lithos **75**, 1-17.

FAURE, F., TROILLIARD, G., MONTEL, J.M. & NICOLLET, C. (2001): Nano-petrographic investigation of a mafic xenolith (Maar de Beaunit, Massif Central, France). *Eur. J. Mineral.* **13**, 27-40.

FERRI, F., BURLINI, L., CESARE, B. & SASSI, R. (2007): Seismic properties of lower crustal xenoliths from El Hoyazo (SE Spain): Experimental evidence up to partial melting. *Earth Planet. Sci. Lett.* **253**, 239-253.

FISHER, G.W. (1989): Matrix analysis of metamorphic mineral assemblages and reactions. *Contrib. Mineral. Petrol.* **102**, 69-77.

FOSTER, C.T. (1986) Thermodynamic models of reactions involving garnet in a sillimanite/ staurolite schist. *Mineral. Mag.*, **50**, 427-439.

FRENCH, B.M. (1964): Graphitization of organic material in a progressively metamorphosed Precambrian iron formation. *Science* **146**, 917-918.

GRANT, J.A. (1985): Phase equilibria in partial melting of pelitic rocks. *In:* High Temperature Metamorphism and Crustal Anatexis (J.R. Ashworth and M. Brown, *eds.*) Unwin Hyman, London, 105-144.

GUERNINA, S. & SAWYER, E.W. (2003): Large-scale melt-depletion in granulite terranes; an example from the Archean Ashuanipi Subprovince of Quebec. *J. Metamorphic Geol.* **21**, 181-201.

GUPTA, L.N. & JOHANNES, W. (1982): Genetic model for the stromatic migmatites of the Rantasalmi-Sulkava area, Finland. *J. Petrol*, **27**, 521-539

HOLDAWAY, M.J. (1971): Stability of andalusite and the aluminosilicate phase diagram. *Am. J. Science* **271**, 97-131.

HOLLAND, T. & POWELL, R. (2001): Calculation of phase relations involving haplogranitic melts using an internally consistent thermodynamic dataset. *J. Petrol.* **42**, 673-683.

HOLNESS, M.B. (2008): Decoding migmatite microstructures. *In* Working with Migmatites (E.W. Sawyer & M. Brown, eds.). *Mineral. Assoc. Canada, Short Course* **38**, x-x+22.

HOLTZ, F., BEHRENS, H., DINGWELL, D.B. & JOHANNES, W. (1995): Water solubility in haplogranitic melts. Compositional, pressure and temperature dependence. *Am. Mineral.* **80**, 94-108.

JOHANNES, W. & HOLTZ, F. (1996): Petrogenesis and experimental petrology of granitic rocks. (W. Johannes & F. Holtz, *eds.*) Minerals and Rocks Series Vol. 22. XIII, Berlin: Springer-Verlag, 335 p.

KENAH, C. & HOLLISTER, L.S. (1983) Anatexis in the Central Gneiss Complex, British Columbia. In: Migmatites, Melting and Metamorphism (Atherton and Gribble, *eds.*), Proceedings of the Geochemical Group of the Mineralogical Society, Shiva Geology Series, 142-162.

KRETZ, R., 1983, Symbols for rock-forming minerals: *Am. Mineral*. **68**, 277-279.

KRIEGSMAN, L.M. & HENSEN, B.J. (1998): Back reaction between restite and melt: Implications for geothermobarometry and pressure-temperature paths. *Geology* **26**, 1111-1114.

LE BRETON, N. & THOMPSON, A.B. (1988): Fluid-absent (dehydration) melting of biotite in metapelites in the early stages of crustal anatexis. *Contrib. Mineral. Petrol.* **99**, 226-237.

MONTEL, J.M. & VIELZEUF, D. (1994): Partial melting of metagreywackes. Part 2. Compositions of minerals and melts. *Contrib. Mineral. Petrol.* **128**, 176-196.

NAIR, R. & CHACKO, T. (2002): Fluid-absent melting of high-grade semi-pelites; P-T constraints on orthopyroxene formation and implications for granulite genesis. *J. Petrol.* **43**, 2121-2142.

NIXON, P.H. (1987): Mantle Xenoliths. (P.H. Nixon, *ed.*), New York: John Wiley, 844p.

PATIÑO-DOUCE, A.E. & JOHNSTON, A.D. (1991): Phase equilibria and melt productivity in the pelitic system; implications for the origin of peraluminous granitoids and aluminous granulites. *Contrib. Mineral. Petrol.* **107**, 202-218.

PATTISON, D.R.M. (1992): Stability of andalusite and sillimanite and the Al_2SiO_5 triple point; constraints from the Ballachulish aureole, Scotland. *J. Geology* **100**, 423-446.

PERINI G., CESARE B., GÓMEZ-PUGNAIRE M.T., GHEZZI, S., TOMMASINI S. Armouring effect in decoupling Sr-Nd isotopes during disequilibrium crustal melting: the case study of frozen migmatites from El Hoyazo and Mazarrón, SE Spain. *Eur. J. Mineral*., in press.

ROEDDER, E. (1984): Fluid inclusions (P.H. Ribbe, *ed.*) Rev. Mineral. **12**, 646 p.

RUBIE, D.C. AND BREARLEY, A.J. (1990) A model for rates of disequilibrium melting during metamorphism. In: High Temperature Metamorphism and Anatexis (Ashworth and Brown, *eds*.), Unwin-Hyman Ltd, 57–86.

SALVIOLI MARIANI, E., RENZULLI, A., SERRI, G., HOLM, P.M. & TOSCANI, L. (2005): Glass-bearing crustal xenoliths (buchites) erupted during the Recent activity of Stromboli (Aeolian Islands). *Lithos* **81**, 255-277.

SAWYER, E.W. (1987): The role of partial melting and fractional crystallization determining discordant migmatite leucosome compositions. *J. Petrol.* **28**, 445-473.

SOBOLEV, V.S. & KOSTYUK, V.P. (1975): Magmatic crystallization based on a study of melt inclusions. *Fluid Incl. Res.* **9**, 182-253 (translated from original publication in Russian).

SOLAR, G.S. & BROWN, M. (2001): Petrogenesis of migmatites in Maine, USA; possible source of peraluminous leucogranite in plutons? *J. Petrol.* **42**, 789-823.

TSUCHIYAMA, A. (1986): Melting and dissolution kinetics: application to partial melting and dissolution of xenoliths. *J. Geophys. Res.* **91**, 9395-9406.

VERNON, R.H. (1987) Oriented growth of sillimanite in andalusite, Placitas-Juan Tabo area, New Mexico, U.S.A. *Can. J. Earth Sci.* **24**, 580–590.

VERNON, R.H. (2004): A practical guide to rock microstructure. Cambridge, Cambridge University Press, 594 p.

VERNON, R.H. (2007): Problems in identifying restite in S-type granites of southeastern Australia, with speculations on sources of magma and enclaves. *Can. Mineral.* **45**, 147-178.

VIELZEUF, D. & HOLLOWAY, J.R. (1988): Experimental determination of the fluid-absent melting relations in the pelitic system. *Contrib. Mineral. Petrol.* **98**, 257-276.

WEBSTER, J.D. (2006): Melt inclusions in Plutonic Rocks (J.D. Webster *ed.*) Min. Assoc. Canada, Short Course **36**.

WHITE, R. W., POWELL, R., AND HOLLAND, T. J. B. (2007) Progress relating to calculation of partial melting equilibria for metapelites. *J. Metamorphic Geol*. **25**, 511–527

ZECK, H.P. (1970): An erupted migmatite from Cerro de Hoyazo, SE Spain. *Contrib. Mineral. Petrol.* **26**, 225-246.